International Journal of Biological Macromolecules 265 (2024) 130712

Contents lists available at ScienceDirect

International Journal of Biological Macromolecules

journal homepage: www.elsevier.com/locate/ijbiomac

Lichen pectin-containing polysaccharide from *Xanthoria elegans* and its ability to effectively protect LX-2 cells from H_2O_2-induced oxidative damage

Zheng Zhou [a,b,c], Guoqiang Li [a,b,c], Liang Gao [a,b,c], Yubi Zhou [b,c], Yuancan Xiao [a,b,c], Hongtao Bi [a,c,*], Hongxia Yang [a,b,c,**]

[a] Qinghai Provincial Key Laboratory of Tibetan Medicine Pharmacology and Safety Evaluation, Northwest Institute of Plateau Biology, Chinese Academy of Sciences, Xining 810008, China
[b] CAS Key Laboratory of Tibetan Medicine Research, Northwest Institute of Plateau Biology, Xining 810001, China
[c] University of Chinese Academy of Sciences, Beijing 100049, China

ARTICLE INFO

Keywords:
Antioxidant activity
Hepatic stellate cells
Lichen
Pectin
Xanthoria elegans

ABSTRACT

Xanthoria elegans, a drought-tolerant lichen, is the original plant of the traditional Chinese medicine "Shihua" and effectively treats a variety of liver diseases. However, thus far, the hepatoprotective effects of polysaccharides, the most important chemical constituents of *X. elegans*, have not been determined. The aim of this study was to screen the polysaccharide fraction for hepatoprotective activity by using free radical scavenging assays and a H_2O_2-induced Lieming Xu-2 cell (LX-2) oxidative damage model and to elucidate the chemical composition of the bioactive polysaccharide fraction. In the present study, three polysaccharide fractions (XEP-50, XEP-70 and XEP-90) were obtained from *X. elegans* by hot-water extraction, DEAE-cellulose anion exchange chromatography separation and ethanol gradient precipitation. Among the three polysaccharide fractions, XEP-70 exhibited the best antioxidant activity in free radical scavenging capacity and reducing power assays. Structural studies showed that XEP-70 was a pectin-containing heteropolysaccharide fraction that was composed mainly of (1 → 4)-linked and (1 → 4,6)-linked α-D-Glc*p*, (1 → 4)-linked α-D-Gal*p*A, (1 → 2)-linked, (1 → 6)-linked and (1 → 2,6)-linked α-D-Man*p*, and (1 → 6)-linked and (1 → 2,6)-linked β-D-Gal*f*. Furthermore, XEP-70 exhibited effectively protect LX-2 cells against H_2O_2-induced oxidative damage by enhancing cellular antioxidant capacity by activating the Nrf2/Keap1/ARE signaling pathway. Thus, XEP-70 has good potential to protect hepatic stellate cells against oxidative damage.

1. Introduction

In biological systems, elevated levels of reactive oxygen species (ROS) and low levels of antioxidant mechanisms can lead to oxidative stress in cells [1]. Under normal conditions, ROS are produced in response to mitochondrial oxygen metabolism and are involved in cellular signaling. However, excessive ROS production and impaired antioxidant capacity can induce structural cellular damage and destroy tissue. This change is thought to be associated with the development of many chronic diseases, such as inflammation, diabetes, cancer and aging [2,3]. Hydrogen peroxide (ROS, a nonfree radical) is one of the main causes of oxidative stress in cells and is commonly used to assess antioxidant capacity and cellular ROS scavenging capacity [4].

The liver is an important organ for detoxification and metabolism in the body, and studies have shown that liver cell damage is closely associated with increased ROS, while oxidative stress is thought to be one of the pathological mechanisms contributing to the development and progression of various liver diseases [5,6]. Therefore, antioxidants are considered good agents for the treatment of liver diseases. Although synthetic antioxidants are able to prevent the radical chain reactions of oxidation, they cause almost unavoidable side effects and might be responsible for liver damage and carcinogenesis [6]. Thus, it is essential to develop natural antioxidants that can protect the human body from

* Corresponding author at: Qinghai Provincial Key Laboratory of Tibetan Medicine Pharmacology and Safety Evaluation, Northwest Institute of Plateau Biology, CAS, 23 Xinning Road, Xining 810008, China.
** Correspondence to: H.Yang, CAS Key Laboratory of Tibetan Medicine Research, Northwest Institute of Plateau Biology, Xining 810001, China.
E-mail addresses: bihongtao@hotmail.com (H. Bi), hxyang@nwipb.cas.cn (H. Yang).

https://doi.org/10.1016/j.ijbiomac.2024.130712
Received 14 December 2023; Received in revised form 11 February 2024; Accepted 5 March 2024
Available online 11 March 2024

Abbreviations

ABTS	2,2′-Azinobis [3-ethylbenzothiazoline-6-sulfonic acid]-diammonium salt
ANOVA	analysis of variance
CAT	catalase
CCK-8	Cell Counting Kit-8
DEAE	diethylaminoethyl
DPPH	2,2-Diphenyl-1-picrylhydrazyl
GCLC	glutamate-cysteine ligase catalytic subunit
GCLM	glutamate-cysteine ligase modifier subunit
GSH	glutathione
HO-1	heme oxygenase 1
LDH	lactate dehydrogenase
MDA	malondialdehyde
NMR	nuclear magnetic resonance
NQO1	NAD(*P*)H quinone oxidoreductase 1
PMP	1-phenyl-3-methyl-5-pyrazolone
ROS	reactive oxygen species
SOD	superoxide dismutase
SEM	scanning electron microscope
T-AOC	total antioxidant capacity
XEP	*Xanthoria elegans* polysaccharide

free radicals and retard the progression of liver diseases, and medicinal plants have been shown to be good resources of natural antioxidants [7–9].

In recent years, polysaccharides have attracted increasing amounts of attention owing to their diverse health-promoting effects, nontoxicity, extensive accessibility and renewability [10–12]. In recent years, polysaccharides from natural sources have been linked to antioxidant effects in both *in vitro* chemical and biological models and found to play key roles in regulating excessive oxidative stress [13–15]. The reported structures, which are claimed to act as antioxidants, include chitosan, pectic polysaccharides, glucans, mannoproteins, alginates, fucoidans, and many others from all types of biological sources [10–17]. However, compared with those of natural polysaccharides from herbs and woody plants, less research has been conducted on the antioxidant and hepatoprotective effects of natural polysaccharides from lichens.

Xanthoria elegans, a common drought-tolerant lichen, belongs to the *Teloschistaceae* family and is widely distributed in cool-temperate Europe, North America and East Asia [18]. *X. elegans* is the original plant of the traditional Chinese medicine "Shihua" and is used to treat diseases such as blurred vision, waist and knee pain, and hematemesis. The main effect of this treatment is to nourish the liver and kidney. There are many pharmacological components in *X. elegans*, including phenolic compounds, organic acids, polysaccharides and volatile oils, which have pharmacological activities, such as antiulcer, anticancer, antioxidative and antiviral activities [19–23]. However, the chemical composition and antioxidant and hepatoprotective effects of polysaccharides, which are the most important chemical constituents of *X. elegans*, have not been fully elucidated. Thus, the aim of this study was to screen the polysaccharide fraction with hepatoprotective activity by using free radical scavenging assays and a hydrogen peroxide-induced Lieming Xu-2 cell (LX-2) oxidative damage model and to elucidate the chemical composition of the bioactive polysaccharide fraction by using monosaccharide composition, FT-IR, NMR, SEC and AFM analyses.

2. Materials and methods

2.1. Materials and reagents

Xanthoria elegans was collected from the Laji Mountain habitat (101°33′E, 36°19′N; 3820 m altitude) in Qinghai Province, China. It was identified by L.S. Wang, Kunming Institute of Botany, Chinese Academy of Sciences.

DEAE cellulose was obtained from Yuanye BioTechnology (Shanghai, China). BCA and T-AOC were obtained from Beyotime (Shanghai, China). CAT, MDA, ROS, GSH, LDH and SOD were acquired from Nanjing Jiancheng Bioengineering (Nanjing, China). LX-2 cells (CL-0560) and DMEM (PM1500210) were obtained from Procell (Wuhan, China), and FBS (10099-141C) was obtained from Gibco (New York, USA). All antibodies used in the experiments were obtained from Abcam (Cambridge, UK), except for the goat anti-rabbit (HRP) antibody (AS1107), which was purchased from Aspen (Wuhan, China). All the other chemical reagents were of analytical grade.

2.2. Extraction and purification of XEP

Xanthoria elegans (1 kg) was extracted three times with boiling distilled water (10*L*) and concentrated to a small volume of approximately 1 L at 95 °C [24,25], after which the polysaccharides were precipitated with 80 % ethanol. The extracts were detached by centrifugation at 4500 rpm for 15 min (3-18 K, SIGMA, Germany) and freeze-dried (FD-1A-80, BIOCOOL, Beijing, China). *X. elegans* polysaccharide (XEP) was collected.

XEP (200 mg) was dissolved in distilled water (5 mL) and loaded into a DEAE-cellulose column (20 mm × 20 cm) with distilled water (200 mL) and 0.5 M NaCl solution (200 mL) at a flow rate of 1.8 mL/min [26]. The eluents were collected in 7.4-mL aliquots in each tube, and the sugar content was measured using the phenol–sulfuric acid assay. Following collection, the major fractions were dialyzed with distilled water for 24 h (cutoff MW 3500 Da) and running water for 24 h before being lyophilized. The 0.5 M NaCl-eluted polysaccharide was named XEP-1.

XEP-1 was dissolved in distilled water (10 mg/mL), and anhydrous alcohol was slowly added to the XEP solution (10 mg/mL) to a final ethanol concentration of 50 % (*v*/v). After the solution was incubated for 48 h at 4 °C, the precipitates (XEP-50) were collected by centrifugation at 12,000 rpm for 15 min and subsequently dried under vacuum [27,28]. Similar results were achieved for subfractions XEP-70 and XEP-90 with final ethanol concentrations of 70 % and 90 %, respectively. The distilled water used in the experiment was prepared with a multieffect tubular water distiller (LD500–5; Guanyu Environmental Protection Equipment Co., Ltd., Hebei, China), and the electrical conductivity was 2 μs/cm.

2.3. Structural characterization of XEP samples

2.3.1. Homogeneity and molecular weight determination

SEC-MALLS-RI was used to measure the molecular weight [29]. Shodex OH-pak SB-805, 804 and 803 columns (8 mm ID × 300 mm; Showa Denko K.K., Tokyo, Japan) were used in tandem. XEP (1 mg) was dissolved in 1 mL of 0.1 $NaNO_3$ aqueous solution, and the solution (0.45 μm) was passed through the membrane. Detection was performed at a column temperature of 45 °C, an injection volume of 100 μL, a mobile phase of 0.02 % NaN_3 and 0.1 % $NaNO_3$, and a flow rate of 0.4 mL/min. ASTRA 6.1 (Wyatt Technology, USA) was used for data processing.

2.3.2. Chemical composition analysis

Six monosaccharides were used as references, and the phenol-H_2SO_4 method was used to calculate the total carbohydrate content by combining the correction factors of the monosaccharides [30]. Galacturonic acid was used as a reference to quantify the amount of uronic acid using the *m*-hydroxydiphenyl colorimetric method [29]. Using bovine serum albumin as a reference, the amount of protein was determined using the Coomassie brilliant blue method [31].

2.3.3. Monosaccharide composition analysis

The monosaccharide compositions of the polysaccharide samples

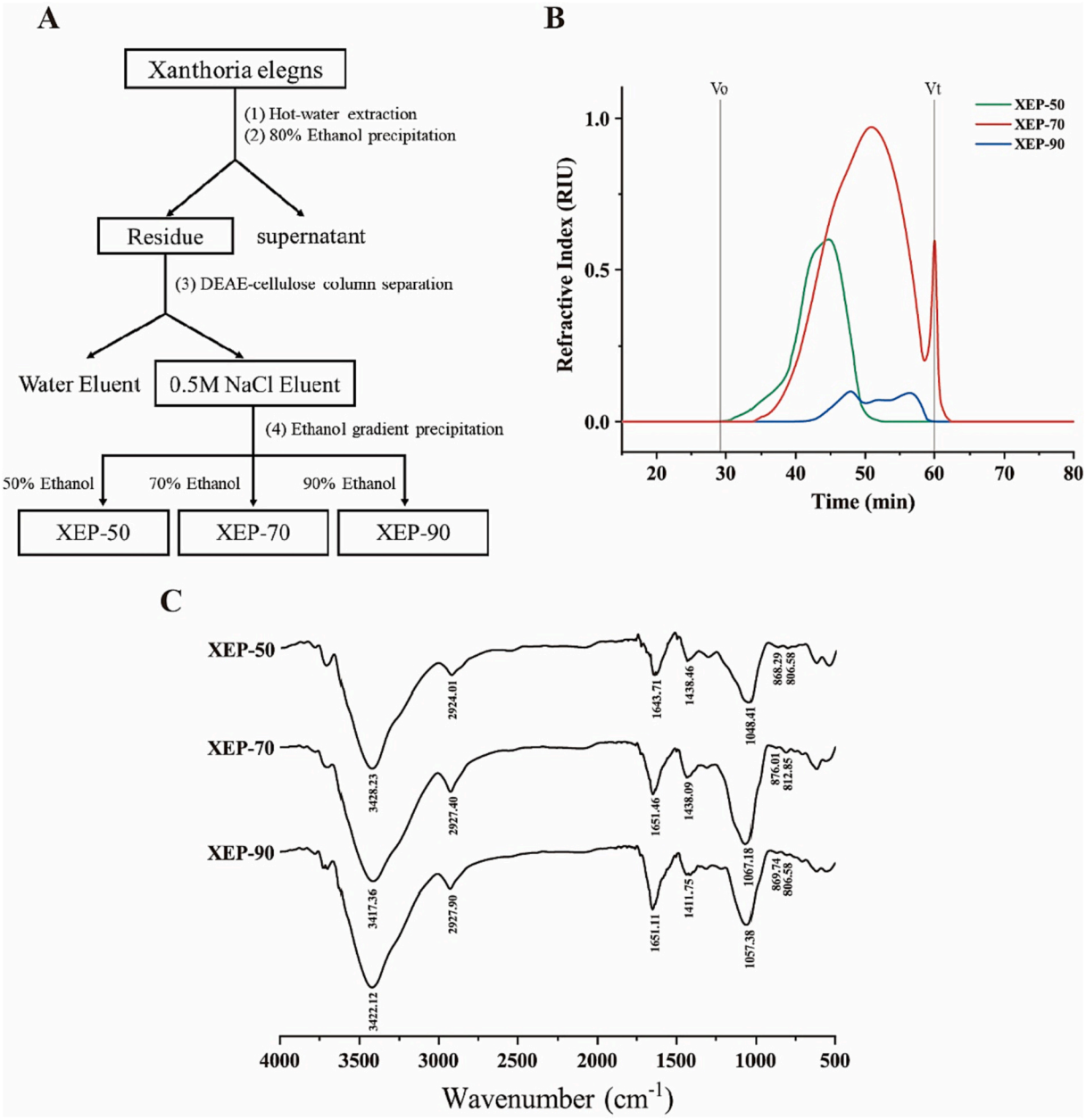

Fig. 1. (A) Process of extraction, isolation and purification of *Xanthoria elegans* polysaccharide. (B) Elution profiles of *Xanthoria elegans* polysaccharide fractions on Ohpak SB columns. (C) FT-IR spectra of *Xanthoria elegans* polysaccharide fractions.

were identified by our previously reported approach [31]. XEP (3 mg) was dissolved in 1 mL of 2 M trifluoroacetic acid (TFA) and sealed in an ampoule for 2 h at 120 °C. The remaining TFA was then removed with anhydrous ethanol, and the solution was evaporated to dryness below 70 °C. 0.5 mL of NaOH (0.3 M) and 0.5 mL of 1-phenyl-3-methyl-5-pyrazolone (PMP, 0.5 M) were used to derivate the polysaccharide hydrolysate at 70 °C for 30 min. The mixture was extracted three times with chloroform after being neutralized with 0.5 mL of 0.3 M HCl. The derivative was tested using an Ultimate 3000 UHPLC system and a Kinetex C18 column (100 × 4.6 mm i.d.) with a guard column. UV absorbance at a wavelength of 245 nm was used to record this process.

2.3.4. FT-IR spectroscopy analysis [31]

The FT-IR spectra of the polysaccharide samples were recorded using a Fourier transform infrared spectrophotometer (Nicolet-IS50, US). The samples (2 mg) were ground with KBr powder, condensed into pellets, and then recorded on an FT-IR spectrometer (resolution, 4 cm^{-1}) in the frequency range of 4000–400 cm^{-1} (mid-infrared region).

2.3.5. Scanning electron microscopy (SEM) analysis [31]

A small amount of the XEP-70 sample was placed on conductive adhesive and sprayed with gold. SEM images of XEP-70 were recorded on a ZEISS GeminiSEM 300 (ZEISS, Germany). The images were viewed in a high-vacuum setting at a voltage of 3.0 kV with 400- and 4000-fold magnification.

2.3.6. Atomic force microscopy (AFM) analysis [31]

AFM was used to examine the morphological characteristics of XEP-70 (Bruker Dimension Icon, Germany). XEP-70 was dissolved in ultrapure water (5 g/mL). Next, 5 μL of the polysaccharide solution was placed on the exterior of a pristinely cleaved mica sheet and allowed to dry at room temperature. The photographs were taken at a scan rate of 1.0 Hz and a scan size of 600 nm.

Table 1
The yield, total sugar content, protein content, uronic acid content and monosaccharide composition of *Xanthoria elegans* polysaccharides.

Fraction	Yield (%)	Total sugar content (%)	Protein content (%)	Uronic acid content (%)	Monosaccharide composition (%)					
					Man	GalUA	Glc	Gal	Xyl	Ara
XEP-50	0.57 ± 0.03$^{\#}$	89.00 ± 0.19$^{\#}$	0.91 ± 0.02	1.13 ± 0.09$^{\#}$	55.00 ± 2.13$^{\#}$	2.56 ± 0.22$^{\#}$	26.48 ± 1.69$^{\#}$	13.96 ± 2.07$^{\#}$	2.00 ± 0.43$^{\#}$	ND
XEP-70	0.83 ± 0.05*	99.05 ± 0.15*	ND	13.09 ± 0.31*	39.28 ± 2.12*	16.09 ± 1.03*	17.56 ± 1.74*	23.20 ± 1.94*	3.87 ± 0.85*	ND
XEP-90	0.37 ± 0.03*$^{\#}$	82.42 ± 0.11*$^{\#}$	ND	7.22 ± 0.27*$^{\#}$	32.63 ± 1.25*	8.64 ± 0.54*$^{\#}$	15.65 ± 1.93*	34.67 ± 2.25*$^{\#}$	1.17 ± 0.61$^{\#}$	7.24 ± 0.03

Each value represents the mean ± SD (n = 6). Significant differences were evaluated using Student's t-test; *$p < 0.05$ *vs* XEP-50; #$p < 0.05$ *vs* XEP-70.

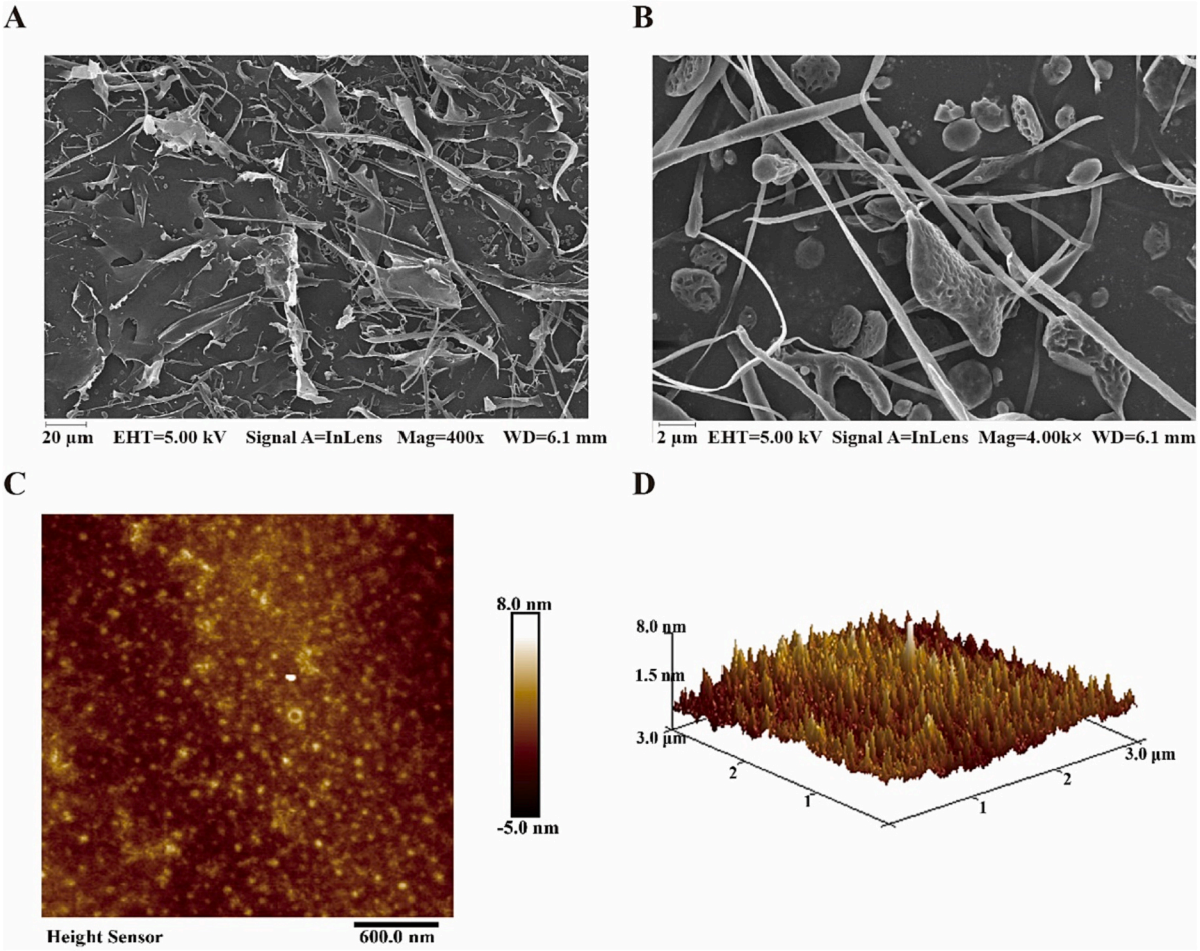

Fig. 2. SEM and AFM images of XEP-70. SEM images, A: 400×; B: 4000×; AFM images, C: Two-dimensional image; D: Three-dimensional image.

2.3.7. Nuclear magnetic resonance (NMR) analysis of XEP-70 [31]

XEP-70 (20 mg) was dissolved in D_2O (99.8 % D, 0.5 mL), freeze-dried, redissolved in D_2O (0.5 mL), and centrifuged to remove excess sample. Then, the aqueous solution of XEP-70 was transferred to an NMR tube (177.8 × 5.0 mm o.d.). NMR analyses, including ^{1}H NMR and ^{13}C NMR, were performed using a Bruker 5 mm broadband observation probe at 20 °C with a Bruker Avance 600 MHz spectrometer (Germany) operating at 600 MHz for ^{1}H and 150 MHz for ^{13}C. All the experiments were recorded using standard Bruker software.

2.4. Free radical scavenging capacity and reducing power assays

2.4.1. DPPH free radical scavenging activity test [32]

DPPH was dissolved in anhydrous ethanol (0.2 mM), and 2 mL of DPPH solution was mixed with 2 mL of the three polysaccharides at different concentrations (0.125–4 mg/mL). After the mixture had reacted for 35 min in the dark, the absorbance of the DPPH free radicals was recorded at 517 nm, which was repeated 4 times.

The clearance rate was calculated as DPPH = $[1-(A_1-A_0)/A_2]*100$ %.

where A_0 is the absorbance of deionized water replacing polysaccharide solution, A_1 is the absorbance of polysaccharide solution, and A_2 is the absorbance of deionized water instead of DPPH or other reagents.

2.4.2. ABTS free radical scavenging activity test [33]

For the preparation of the ABTS experimental reagent, Na_2HPO_4 and NaH_2PO_4 were dissolved in deionized water (50 mM PBS). Other chemical reagents were dissolved in PBS. Using Trolox as a reference, ABTS (5 mM), HRP (1 μM), H_2O_2 (0.018 %) and PBS (50 mM) were added to the three polysaccharide solutions (0.125–4 mg/mL). After the

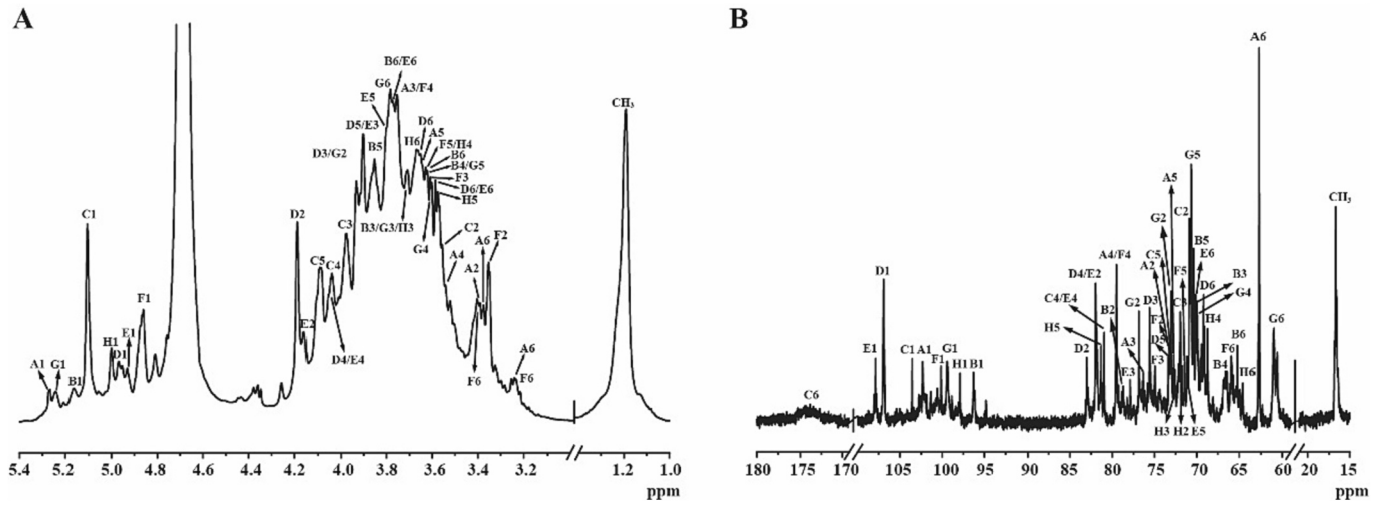

Fig. 3. NMR spectra of XEP-70. (A) ^{1}H NMR spectrum (600 MHz). (b) ^{13}C NMR spectrum (150 MHz); solvent: D_2O, temperature: 20 °C.

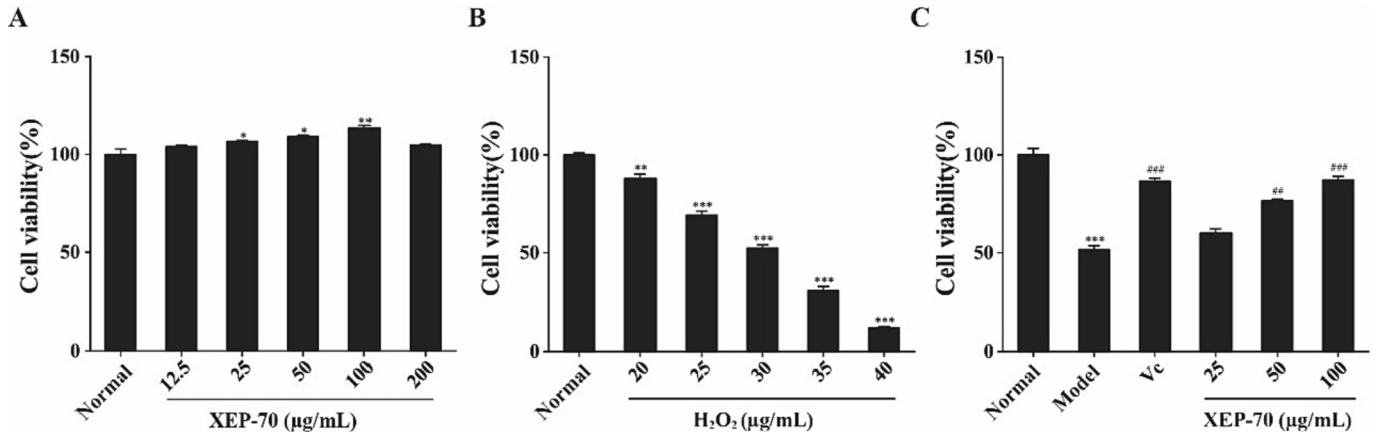

Fig. 4. Effects of XEP-70 and H_2O_2 on the viability of LX-2 cells.

mixture had reacted for 10 min in the dark, the absorbance was recorded at 730 nm, which was repeated 4 times.

The clearance rate was calculated as $ABTS = (1 - A_1/A_0)*100\%$

where A_0 is the absorbance of deionized water replacing the polysaccharide solution and A_1 is the absorbance of the polysaccharide solution.

2.4.3. Superoxide free radical scavenging activity test [34]

NBT, NADH and PMS were dissolved in deionized water, and 1 mL each of NBT (156 μmol/L), NADH (468 μmol/L) and PMS (60 μmol/L) was added to 1 mL of the three polysaccharide solutions at different concentrations (0.125–4 mg/mL). After the mixture had reacted for 5 min in a water bath at 25 °C, the absorbance was recorded at 560 nm, which was repeated 4 times.

The clearance rate was $O^{2-} = [1 - (A_1 - A_2)/A_0]*100\%$

where A_0 is the absorbance of deionized water replacing polysaccharide solution, A_1 is the absorbance of polysaccharide solution, and A_2 is the absorbance of deionized water instead of NBT or other reagents.

2.4.4. Hydroxyl free radical scavenging activity test [35]

The hydroxyl radical scavenging experiment was based on a previous method with some modifications. Then, 0.5 mL each of ferrous sulfate (7.5 mM), salicylic acid (5 mM) and hydrogen peroxide (10 mM) were added sequentially to 0.5 mL of the three polysaccharide solutions at different concentrations (0.125–4 mg/mL). Finally, 2 mL of deionized water was added to each mixed solution. After the mixture had reacted for 20 min in a water bath at 37 °C, the absorbance was recorded at 510 nm, which was repeated 4 times.

The clearance rate was calculated as $OH^{-} = [1 - (A_1 - A_2)/A_0]*100\%$

where A_0 is the absorbance of deionized water replacing polysaccharide solution, A_1 is the absorbance of polysaccharide solution, and A_2 is the absorbance of deionized water instead of $FeSo_4$ or other reagents.

2.4.5. Reducing power test [36]

The determination of reducing power was based on a modification of previous methods. The three polysaccharides were dissolved in 0.2 M phosphate buffer (pH 6.6), and 2.5 mL of different concentrations of polysaccharide solution (0.125–4 mg/mL) was mixed with 2.5 mL of potassium ferricyanide (1 % *w/v*). After the mixture had reacted for 20 min in a water bath at 50 °C, 2.5 mL of trichloroacetic acid (10 % w/v) was added, and the mixture was mixed and centrifuged (3000 rpm for 20 min). Then, 2.5 mL of the supernatant from each solution was added to 2.5 mL of deionized water and 250 μL of ferric chloride (0.1 % w/v) and incubated for 10 min. The absorbance was recorded at 700 nm, which was repeated 4 times.

The reducing power = A_1*100%

Table 2
^{1}H and ^{13}C NMR chemical shifts for residues A-H of XEP-70.

Residue	Chemical shift (ppm)						
	H1/C1	H2/C2	H3/C3	H4/C4	H5/C5	H6,H'6/C6	-CH_3
A	5.27	3.39	3.75	3.52	3.65	3.28, 3.37	
→4)-α-D-Glc*p*-(1→	102.3	73.04	75.58	79.51	72.62	62.73	
B	5.16	4.04	3.71	3.62	3.85	3.63,3.78	
→2,6)-α-D-Man*p*-(1→	96.3	77.97	69.44	66.58	70.09	65.9	
C	5.11	3.54	3.98	4.00	4.11	–	1.19
→4)-α-D-Gal*p*A-(1→	103.55	70.88	71.95	80.97	72.75	173.82	16.68
D	4.97	4.19	3.92	4.09	3.9	3.59, 3.66	
→2,6)-β-D-Gal*f*-(1→	106.93	83.03	75.21	81.94	73.36	68.9	
E	4.81	4.16	3.9	4.09	3.81	3.78, 3.59	
→6)-β-D-Gal*f*-(1→	107.88	81.94	77.89	80.97	71.17	69.93	
F	4.93	3.35	3.61	3.75	3.64	3.2, 3.4	
→4,6)-α-D-Glc*p*-(1→	100.14	73.22	74.96	79.51	71.44	66.36	
G	5.24	4.04	3.71	3.6	3.62	3.86	
→2)-α-D-Man*p*-(1→	99.39	76.85	72.73	69.19	70.11	61	
H	5.00	3.92	3.71	3.64	3.56	3.69	
→6)-α-D-Man*p*-(1→	97.89	72.12	72.6	68.72	81.32	65.2	

where A_1 is the absorbance of the polysaccharide solution.

2.5. The antioxidant effects of XEP on LX-2 cells

2.5.1. Culture of LX-2 cells

LX-2 cells were grown in high-glucose DMEM supplemented with 20 % (*v*/v) FBS, 1 % (v/v) streptomycin, and penicillin at 37 °C in an incubator with humidified 5 % CO_2 [37].

2.5.2. The toxicity test of XEP-70 [38]

LX-2 cells were seeded in a 96-well plate at a density of 5×10^3 cells/well. According to the reported safe dose range of polysaccharides for LX-2 cells [39,40], different concentrations of XEP-70 (12.5, 25, 50, 100 and 200 μg/mL) were added to these wells and incubated for 24 h. CCK-8 reagent was added to each well, after which the plate was cultured for another hour, after which the absorbance was detected.

2.5.3. Screening the concentration of H_2O_2 [41]

LX-2 cells were seeded in a 96-well plate at a density of 5×10^3 cells/well. In accordance with the reported doses of H_2O_2 that cause oxidative damage in LX-2 cells [41,42], different concentrations of H_2O_2 (20, 25, 30, 35 and 40 μg/mL) were added to these wells, and the cells were incubated for 24 h. CCK-8 reagent was added to each well, after which the plates were cultured for another hour to determine the absorbance.

2.5.4. The antioxidant activities of LX-2 [40]

LX-2 cells were seeded in a 96-well plate at a density of 5×10^3 cells/well. According to the reported effective dose range of polysaccharide against oxidative damage [10–17,33,40] and the results of the cytotoxicity test of XEP-70 in LX-2 cells, media containing different concentrations of XEP-70 (25, 50 and 100 μg/mL) were added to these wells and incubated for 24 h. After removing the drug-containing medium by centrifugation, media containing H_2O_2 (30 μg/mL) was added to stimulate the cells for 24 h, after which the CCK8 test was performed.

2.5.5. Antioxidase activities and metabolism content-test [33]

LX-2 cells were seeded in a 6-well cell plate at a density of 2×10^5 cells/well. Then, medium containing Vc (100 μg/mL) was added to the wells of the positive control group, and medium containing XEP-70 (25, 50 or 100 μg/mL) was added to the wells of the experimental groups. After incubating for 24 h, the drug-containing medium was removed by centrifugation. Then, medium containing H_2O_2 (30 μg/mL) was added to the wells of the model control, positive control and experimental groups. After stimulating for 24 h, the cells were washed with PBS three times and then lysed in RIPA lysis buffer (Beyotime, Shanghai, China). The protein content in the cell lysates was determined using a BCA kit. After the cells were collected and processed, the activities of T-AOC, ROS, LDH, CAT, GSH and SOD and the content of MDA in each group were detected according to the manufacturer's recommendations.

2.5.6. Western blotting [43]

The cells were collected and processed as described in Section 2.5.5. The protein concentrations of the samples were measured by an Enhanced BCA Protein Assay Kit (Beyotime, Shanghai, China). All the samples in the experiment were normalized to an equal protein concentration (20 ng/μL) and then denatured. Protein lysates were separated by 10 % SDS–PAGE electrophoresis and transferred to PVDF membranes, followed by the addition of blocking solution at room temperature for 1 h. The blocking solution was removed, and prediluted specific primary antibodies were added overnight at 4 °C. The diluted secondary antibody was added, and the mixture was incubated at room temperature for 30 min. Luminescence development was performed using an enhanced chemiluminescence (ECL) kit, followed by exposure in a dark room and development and fixation.

2.6. Statistical analysis

All the experimental data are expressed as the mean ± standard deviation (SD) of six replicates and were subsequently analyzed by an independent sample *t*-test using GraphPad Prism 8.6.0 software to determine the significance of the treatment sets. Differences with a p value <0.05 were considered to indicate statistical significance.

3. Results

3.1. Extraction and purification of polysaccharide fractions

As shown in Fig. 1A, *Xanthoria elegans* was subjected to hot water extraction and 80 % ethanol precipitation to obtain the crude polysaccharide XEP in 8.62 % yield. The XEP was further purified by a DEAE anion change column into the 0.5 M NaCl fraction XEP-1 (2.48 % yield). Then, XEP-1 was subjected to sequential ethanol precipitation, and three subfractions were obtained, which were termed XEP-50 (0.57 % yield), XEP-70 (0.83 % yield) and XEP-90 (0.37 % yield).

3.2. Molecular weight distribution and homogeneity analysis

As shown in Fig. 1B, the molar masses of the three polysaccharides were determined by a refractive index detector. XEP-50 had only one elution peak with an MW of 322.25 kDa, XEP-70 had one main elution peak with an MW of 430.98 kDa, and XEP-90 had two elution peaks with an MW of 76.36 kDa.

Table 3
DPPH free radical scavenging capacity of *Xanthoria elegans* polysaccharides.

Group dose (mg/mL)	Scavenging rate (%)			
	Vc	XEP-50	XEP-70	XEP-90
0.125	84.67 ± 0.77*#&	3.39 ± 1.31	6.05 ± 0.82	4.16 ± 0.73
0.25	96.43 ± 0.42*#&	7.24 ± 1.26#	13.72 ± 0.27*	10.6 ± 0.9
0.5	97.27 ± 0.31*#&	15.15 ± 2.1#&	25.83 ± 0.85*	22.71 ± 1.84*
1	98.12 ± 0.01*#&	26.62 ± 1.53#&	40.96 ± 0.96*	37.28 ± 1.45*
2	98.21 ± 0.16*#&	33.96 ± 1.20#&	54.02 ± 0.42*	50.14 ± 0.73*
3	98.22 ± 0.13*#&	38.38 ± 0.72#&	63.10 ± 0.87*&	57.24 ± 0.46*#
4	98.40 ± 0.31*#&	40.17 ± 0.96#&	70.39 ± 1.43*&	61.78 ± 0.60*#

Each value represents the mean ± SD ($n = 6$). Significant differences were evaluated using Student's *t*-test; $^{*}p < 0.05$ *vs* XEP-50; $^{\#}p < 0.05$ *vs* XEP-70; $^{\&}p < 0.05$ *vs* XEP-90.

Table 4
ABTS free radical scavenging capacity of *Xanthoria elegans* polysaccharides.

Group dose (mg/mL)	Scavenging rate (%)			
	Vc	XEP-50	XEP-70	XEP-90
0.125	23.99 ± 0.61*#&	0.63 ± 0.24	0.63 ± 0.28	0.53 ± 0.15
0.25	53.32 ± 0.68*#&	0.97 ± 0.47	1.2 ± 0.42	1.17 ± 0.21
0.5	99.13 ± 0.20*#&	1.57 ± 0.50	3.7 ± 0.39	3.07 ± 0.58
1	100 ± 0.00*#&	3.73 ± 0.71#&	8.1 ± 0.77*	6.54 ± 0.57*
2	100 ± 0.00*#&	5.56 ± 0.64#&	14.84 ± 0.82*	11.87 ± 0.77*
3	100 ± 0.00*#&	8.13 ± 0.90#&	22.27 ± 1.01*	18.14 ± 0.95*
4	100 ± 0.00*#&	10.3 ± 0.77#&	30.44 ± 0.76*&	25.38 ± 0.69*#

Each value represents the mean ± SD ($n = 6$). Significant differences were evaluated using Student's *t*-test; $^{*}p < 0.05$ *vs* XEP-50; $^{\#}p < 0.05$ *vs* XEP-70; $^{\&}p < 0.05$ *vs* XEP-90.

3.3. Preliminary characterization of XEP-50, XEP-70 and XEP-90

3.3.1. Chemical composition analysis

The chemical composition and yield of each polysaccharide fraction from *Xanthoria elegans* are summarized in Table 1. The total carbohydrate contents of XEP-50, XEP-70 and XEP-90 were 89.00 %, 99.05 % and 82.42 %, respectively. The uronic acid contents of XEP-50, XEP-70 and XEP-90 were 1.13 %, 13.09 % and 7.22 %, respectively. According to the protein assay results, 0.91 % of the protein was present in XEP-50, and no protein was detected in XEP-70 or XEP-90.

3.3.2. Monosaccharide composition analysis

Table 1 shows that XEP-50 contained mainly mannose (55.00 %), galacturonic acid (2.56 %), glucose (26.48 %), galactose (13.96 %) and xylose (2.00 %); XEP-70 contained mainly mannose (39.28 %), galacturonic acid (16.09 %), glucose (17.56 %), galactose (23.20 %) and xylose (3.87 %); and XEP-90 contained mainly mannose (32.63 %), galacturonic acid (8.64 %), glucose (15.65 %), galactose (34.67 %), xylose (1.17 %) and arabinose (7.24 %).

3.3.3. FT-IR analysis

As shown in Fig. 1C, the FT-IR spectra of the purified XEP-50, XEP-70 and XEP-90 fractions showed polysaccharide absorption peaks in the 4000–400 cm^{-1} range. The characteristic strong absorption bands at approximately 3428.23 cm^{-1} (XEP-50), 3417.36 cm^{-1} (XEP-70) and 3422.12 cm^{-1} (XEP-90) represented the stretching vibrations of the O—H bonds [44]. The stretching vibrations of the C—H bonds in the sugar ring were assigned to the peaks at approximately 2924.01 cm^{-1} (XEP-50), 2927.40 cm^{-1} (XEP-70) and 2927.90 cm^{-1} (XEP-90) [45]. The bands at 1643.71 cm^{-1} (XEP-50), 1651.46 cm^{-1} (XEP-70) and 1651.11 cm^{-1} (XEP-90) were attributed to the C═O stretching vibrations of uronic acids [46]. The signals at 1438.46 cm^{-1} (XEP-50), 1438.09 cm^{-1} (XEP-70) and 1411.75 cm^{-1} (XEP-90) were attributed to in-plane bending vibrations of the C—H bond. The bands at 1048.41 cm^{-1} (XEP-50), 1067.18 cm^{-1} (XEP-70) and 1067.38 cm^{-1} (XEP-90) were attributed to the stretching vibrations of the pyranose rings [47]. The bands at 868.29 cm^{-1} (XEP-50), 876.01 cm^{-1} (XEP-70) and 869.74 cm^{-1} (XEP-90) indicated the presence of β-glycosidic linkages in these fractions [48]. The absorption peaks at 868.29 cm^{-1} (XEP-50), 876.01 cm^{-1} (XEP-70) and 869.74 cm^{-1} (XEP-90) are characteristic of mannose [44]. It is worth mentioning that the peaks at approximately 810 and 870 cm^{-1} appear together and represent peaks of the typical β-dominanting configurations, consisting of glucose and mannose in the form of pyranose [49].

3.3.4. SEM analysis of XEP-70

Fig. 2A and B show the surface morphology of XEP-70 in the SEM images. At a magnification of 400×, XEP-70 appeared to be a stable and irregular reticular structure. When the image was magnified to 4000 times, the closed structure was composed of a large number of sheet structures and ribbon fibers.

3.3.5. AFM analysis of XEP-70

In this study, the chain features and thickness of dispersed XEP molecules on the mica substrate surface were observed. Fig. 2C and D show that the AFM image of XEP-70 displayed many chain structures. Morphological analysis revealed that the XEP-70 molecule existed as a flexible chain with an average thickness of 0.863 nm between a single polysaccharide chain (approximately 0.1–1.0 nm). indicating that most branches in the structure of XEP are independent of each other.

3.3.6. NMR analysis of XEP-70

The XEP-70 structure was analyzed using NMR techniques. As shown in Fig. 3A, the region at δ 4.8–5.3 ppm in the ^{1}H NMR spectrum is associated with ectopic protons, in which 8 signals at 5.27, 5.24, 5.16, 5.11, 5.00, 4.97, 4.93 and 4.81 ppm are shown. These signals were named A-H according to the order based on the magnitude of the chemical shifts. The signals present in the δ3.1–4.3 ppm region were considered to be associated with H2-H6. As shown in Fig. 3B, the region at δ 90–110 ppm in the ^{13}C NMR spectrum was associated with anomeric carbons, and 8 anomeric carbon signals were observed, which could be assigned to correspond to the ^{1}H NMR spectra, with A-H signals of 107.88, 106.93, 103.55, 102.30, 100.14, 99.39, 97.89 and 96.30 ppm, while chemical shifts at δ 60–85 ppm were associated with nonanomeric carbons. The signal at 106.93 ppm is characteristic of the anomeric carbons of the β-galactofuranose moiety because of their extremely low field shifts. The signal at 173.82 ppm is attributed to XEP-70 containing galacturonic acid [50].

The signals corresponding to each residue of XEP-70 in the one-dimensional NMR spectra (Fig. 4) were compared with the NMR data in the literature [51–54], and the results are summarized in Table 2. The signals of B (δ5.16/96.3), G (δ5.24/99.39) and H (δ5.00/97.89) represent three different α-mannopyranose residues; the signals of A (5.27/102.30) and F (4.93/100.14) represent two different α-glucopyranose residues; the signals of D (4.97/106.93) and E (4.81/107.88) represent two different galactofuranose residues; and the signals of C (5.11/103.55) are from a galacturonic acid residue. Due to the overabundance of various monosaccharide residues in the one-dimensional NMR spectra, the spectra were too complex; therefore, the next step of linkage and structural speculation was not carried out.

Table 5
Superoxide free radical scavenging capacity of *Xanthoria elegans* polysaccharides.

Group dose (mg/mL)	Scavenging rate (%)			
	Vc	XEP-50	XEP-70	XEP-90
0.125	94.51 ± 0.39*#&	1.78 ± 0.62	3.15 ± 0.66	2.65 ± 0.31
0.25	97.16 ± 0.09*#&	3.42 ± 0.46#	6.18 ± 0.64*	4.48 ± 0.60
0.5	98.41 ± 0.20*#&	6.39 ± 0.99#&	13.2 ± 0.73*	11.58 ± 0.63*
1	98.89 ± 0.05*#&	12.88 ± 0.79#&	24.04 ± 0.76*	22.42 ± 0.53*
2	99.13 ± 0.05*#&	21.23 ± 0.50#&	38.64 ± 0.76*	35.44 ± 0.60*
3	99.23 ± 0.05*#&	27.96 ± 0.62#&	52.40 ± 0.63*&	44.31 ± 0.85*#
4	99.42 ± 0.05*#&	32.60 ± 0.46#&	59.34 ± 0.60*&	50.07 ± 0.56*&

Each value represents the mean ± SD ($n = 6$). Significant differences were evaluated using Student's *t*-test; $^{*}p < 0.05$ *vs* XEP-50; $^{\#}p < 0.05$ *vs* XEP-70; $^{\&}p < 0.05$ *vs* XEP-90.

Table 6
Hydroxyl free radical scavenging capacity of *Xanthoria elegans* polysaccharides.

Group dose (mg/mL)	Scavenging rate (%)			
	Vc	XEP-50	XEP-70	XEP-90
0.125	20.93 ± 0.61*#&	0.97 ± 0.21	2.10 ± 0.41	1.61 ± 0.57
0.25	39.77 ± 0.41*#&	2.08 ± 0.50	4.39 ± 0.77	3.52 ± 0.44
0.5	66.41 ± 0.30*#&	4.40 ± 0.55#&	9.26 ± 0.4*	7.64 ± 0.45*
1	91.4 ± 0.42*#&	7.53 ± 0.77#&	20.64 ± 0.69*	17.12 ± 0.60*
2	98.38 ± 0.06*#&	15.13 ± 0.57#&	34.03 ± 0.49*	32.33 ± 0.46*
3	99.15 ± 0.04*#&	22.24 ± 0.54#&	46.46 ± 0.65*	43.45 ± 0.68*
4	99.45 ± 0.07*#&	25.59 ± 0.67#&	52.14 ± 0.55*	48.48 ± 0.56*

Each value represents the mean ± SD ($n = 6$). Significant differences were evaluated using Student's *t*-test; $^{*}p < 0.05$ *vs* XEP-50; $^{\#}p < 0.05$ *vs* XEP-70; $^{\&}p < 0.05$ *vs* XEP-90.

Generally, polysaccharides are produced by both lichen symbionts. The mycobiont cell wall contains three structurally different polysaccharides, namely, β-glucans, α-glucans, and galactomannans. β-glucans, α-glucans, and galactomannans have linear, lightly substituted, and branched structures. Lichenan, isolichenan, and galactoglucomannans are common examples of β-glucans, α-glucans, and galactomannans typically isolated from various lichen species. In addition to these three basic types of lichen polysaccharides, complex heteroglycans consisting of monosaccharides differing from or in addition to galactose, glucose, and mannose have also been reported [55]. However, in addition to four acid polysaccharides with 0.50 %–0.83 % uronic acid content from *Umbilicaria esculenta* [56], there are no reports on polysaccharides containing pectin from lichens. In the present study, XEP-70 was a pectin-containing heteropolysaccharide fraction comprising 16.09 % galacturonic acid; this fraction was composed mainly of (1 → 4)-linked α-D-Gal*p*A, (1 → 4)-linked and (1 → 4,6)-linked α-D-Glc*p*; (1 → 2)-linked, (1 → 6)-linked and (1 → 2,6)-linked α-D-Man*p*; and (1 → 6)-linked and (1 → 2,6)-linked β-D-Gal*f*. This study provides new insights into the structure of lichen polysaccharides.

3.4. Free radical scavenging capacity and reducing power of X. elegans polysaccharides

The free radical group is an unpaired group in the human body that has strong oxidative properties. Excessive free radicals induce protein denaturation and cell damage and eventually lead to human disease and aging [13–16]. According to the reported effective dose range of polysaccharides for free radical scavenging and reducing power [10–17,33,40], the antioxidant activities of the three polysaccharides were evaluated at doses ranging from 0.125 to 4 mg/mL in this study. The antioxidant activities of the three polysaccharides at different concentrations are depicted in Tables 3–7, including the scavenging radicals (ABTS, DPPH, O^{2-} and OH^{-}) and reducing power. DPPH is a relatively stable free radical that is usually used to evaluate the free radical scavenging activity of natural compounds. The three polysaccharides had good DPPH free radical scavenging ability at concentrations ranging from 0.125 to 4 mg/mL, and the scavenging ability increased with increasing polysaccharide concentration. As shown in Table 3, at the same concentration, the scavenging ability of XEP-70 was better than that of the other two polysaccharides, with a maximum of 70.38 % ± 1.42 %. Similarly, the ABTS scavenging ability of the three polysaccharides is shown in Table 4. The increases in polysaccharide concentration and scavenging ability were synchronized, and the scavenging effect of XEP-70 was significantly greater than that of the other two polysaccharides.

In the human body, superoxide anions are present in certain amounts and are usually harmless, but the product of their combination with hydroxyl radicals (which have extremely strong oxidation properties) can damage cellular DNA, causing oxidative damage to cells and disrupting body functions [15,16]. As shown in Tables 5 and 6, the abilities of the three polysaccharides to scavenge O^{2-} radicals and OH^{-} radicals were similar, and the scavenging ability increased as the polysaccharide concentration increased. The best effect was achieved by XEP-70, which reached a maximum clearance at 4 mg/ml, at 59.34 ± 0.60 % and 52.14 ± 0.55 %, respectively.

The reducing power trends of the three polysaccharides were similar to the free radical scavenging ability trends described above but exhibited less significant differences than did the free radical scavenging ability (Table 7). Therefore, it is known from the above results that all three polysaccharides have certain free radical scavenging and reducing abilities, among which XEP-70 has the strongest antioxidant activity and was selected for subsequent study.

3.5. The antioxidant activity of XEP-70 in LX-2 cells

3.5.1. Concentration screening of H_2O_2 and XEP-70

LX-2 cells and the H_2O_2 oxidative damage model were selected to investigate the antioxidant activity of the XEP-70 polysaccharide fraction. The toxicity of XEP-70 on LX-2 cells at 12.5, 25, 50, 100, 200 and 400 μg/mL was examined, and as shown in Fig. 4A, XEP-70 significantly promoted cellular proliferation at concentrations ranging from 25 to 100 μg/mL ($P < 0.05$). Therefore, we selected 25, 50 and 100 μg/mL XEP-70 for subsequent experiments to evaluate its antioxidant effect on LX-2 cells.

In the present study, H_2O_2 was used to stimulate oxidative damage in LX-2 cells. H_2O_2 concentrations ranging from 10 to 40 μg/mL were tested. As shown in Fig. 4B, cell damage started with 20 μg/mL H_2O_2, and cell activity decreased as the concentration increased; therefore, we chose the IC_{50} concentration (30 μg/mL) as the modeling concentration for oxidative damage in LX-2 cells.

Using the XEP-70 polysaccharide fraction to protect oxidative damage in LX-2 cells, as shown in Fig. 4C, different concentrations of XEP-70 were found to protect cells and increase cell activity compared with those in the damage model group, with 100 μg/mL having the greatest effect, which was close to that of the positive control group.

Normal: untreated control cells. Model: Cells were treated with blank medium for 24 h and then treated with medium containing 30 μg/mL H_2O_2 for 24 h. Other groups: cells were treated with medium containing Vc or XEP-70 for 24 h and then treated with medium containing 30 μg/

Table 7
Reducing power of *Xanthoria elegans* polysaccharides.

Group dose (mg/mL)	Reducing power ($A_{700\ nm}$)			
	Vc	XEP-50	XEP-70	XEP-90
0.125	0.53 ± 0.01*#&	0.00 ± 0.00	0.01 ± 0.00	0.01 ± 0.00
0.25	0.89 ± 0.01*#&	0.01 ± 0.00	0.03 ± 0.00	0.01 ± 0.01
0.5	1.46 ± 0.02*#&	0.02 ± 0.00	0.06 ± 0.00	0.03 ± 0.01
1	1.72 ± 0.01*#&	0.04 ± 0.01#	0.11 ± 0.01*&	0.05 ± 0.01
2	1.77 ± 0.01*#&	0.08 ± 0.01#	0.22 ± 0.01*&	0.09 ± 0.01
3	1.79 ± 0.02*#&	0.11 ± 0.01#	0.31 ± 0.01*&	0.15 ± 0.01
4	1.80 ± 0.01*#&	0.14 ± 0.01#&	0.43 ± 0.01*&	0.20 ± 0.01*

Each value represents the mean ± SD (n = 6). Significant differences were evaluated using Student's t-test; *$p < 0.05$ *vs* XEP-50; #$p < 0.05$ *vs* XEP-70; &$p < 0.05$ *vs* XEP-90.

mL H_2O_2 for 24 h. All the data are expressed as the means ± SDs ($n = 6$). *$p < 0.05$, **$p < 0.01$ and ***$p < 0.001$ *vs.* the normal control group; ##p < 0.01 and ###p < 0.001 *vs.* the model control group.

3.5.2. XEP-70 improves LX-2 antioxidant activity

In the present study, the antioxidant activity of LDH, ROS, T-AOC, GSH, SOD, and CAT and the content of MDA were determined in LX-2 cells. As shown in Fig. 5A, XEP-70 significantly reduced the MDA content in cells in a dose-dependent manner ($P < 0.05$), and the changes in LDH and ROS activities are shown in Fig. 5B and C. These trends were similar to the above results. As shown in Fig. 5D-G, the activities of T-AOC, GSH, SOD and CAT in the model group were significantly lower than those in the blank group, but the activity of the above enzymes was reversed and significantly enhanced in a dose-dependent manner in the experimental group with preadded XEP-70 ($p < 0.05$). Taken together, these results indicated that XEP-70 could effectively protect LX-2 cells from oxidative damage caused by H_2O_2 by modulating the activities of antioxidant enzymes.

3.5.3. The Nrf2/Keap1/ARE signaling pathway is activated by XEP-70

Nrf2 is a key regulator of cellular oxidative stress and maintains cellular redox homeostasis. The Nrf2-mediated pathway is induced and activated by electrophilic reagents of different origins and structures. Activated Nrf2 subsequently binds to ARE elements in the nucleus and induces and regulates the expression of many downstream antioxidant factors. Keap1 is a sensor in the oxidative stress pathway; it binds to Nrf2 to form a dimer that negatively regulates Nrf2 and inhibits Nrf2 activity [17,57,58]. Fig. 6A and B shows that H_2O_2 treatment significantly reduced cellular Nrf2 expression in the model group, but pretreatment with XEP-70 significantly reversed this change, as indicated by a significant increase in Nrf2 expression. In contrast, Keap1 expression was increased in the cells of the model group and significantly decreased after pretreatment with XEP-70. The above results suggest that XEP-70 can downregulate Keap1 in the Nrf2-Keap1 dimer in the cellular oxidative pathway and promote the release and upregulation of Nrf2 from the dimer.

3.5.4. Influence on the expression of NQO1, HO-1, GCLC and GCLM in LX-2 cells

HO-1 and NQO1 are important downstream antioxidant enzymes produced by Nrf2 activation and are important expression products of cellular antioxidants. It has been shown that HO-1 protects mitochondria, promotes heme degradation and produces active substances to scavenge ROS [59]. NQO1 can catalyze the electron reduction of various organic compounds and reduce the free radical load in cells [60]. GCLC and GCLM can work together as two subunits from GCL, providing catalytic activity and promoting GSH synthesis, thus enhancing cellular antioxidant capacity [61].

Fig. 6A and B shows that the expression of NQO1, HO-1, GCLC and GCLM was significantly greater after pretreatment with XEP-70 at concentrations of 50 and 100 μg/mL than in the model group ($p < 0.01$); thus, XEP-70 activated Nrf2 in the Nrf2/Keap1/ARE signaling pathway, which was transferred to the nucleus to further promote the expression of NQO1, HO-1, GCLC and GCLM, resulting in a reduction in the oxidative damage caused by H_2O_2 and antioxidant effects.

Normal: untreated control cells. Model: Cells were treated with blank medium for 24 h and then treated with medium containing 30 μg/mL H_2O_2 for 24 h. Other groups: cells were treated with medium containing Vc or XEP-70 for 24 h and then treated with medium containing 30 μg/mL H_2O_2 for 24 h. All the data are expressed as the means ± SDs ($n = 6$). *$p < 0.05$, **p < 0.01 and ***$p < 0.001$ *vs.* the Model control group.

4. Discussion

Lichens are composed of both fungi and algae and form a stable and mutually beneficial complex of organisms that carry out photosynthesis to produce carbohydrates [62]. Approximately 13,500 species of lichens have been identified around the world, approximately 4500 of which have been studied on the basis of low-molecular-weight compounds, compared to <100 high-molecular-weight compounds such as polysaccharides. There are three main structures of lichen polysaccharides that have been studied: α-glucan, β-glucan and galactomannan. Various pharmacological activities of lichens, such as antiviral, antitumor, antibacterial, analgesic and antipyretic activities, have been demonstrated. Lichen polysaccharide is an important active ingredient in lichens [63].

According to the results of the free radical scavenging assay, XEP-70 exhibited the strongest scavenging ability, followed by XEP-90 and XEP-50. This result is related to its uronic acid content, which has previously been shown to reduce hydroxyl radical synthesis by chelating Fe^{2+} in polysaccharides and increasing reducing power, while the aldehyde and ketone groups in uronic acids are thought to facilitate the separation of hydrogen from O—H bonds [64,65]. Huang et al. reported that five polysaccharides were isolated from *Inonotus obliquus*, and all four polysaccharides containing uronic acid (7.5 %–23.3 %) had greater radical scavenging capacities than those without uronic acid [66]. In addition to the uronic acid content, the antioxidant capacity of polysaccharides may be related to molecular weight, as the antioxidant activity of polysaccharides increases with increasing molecular weight, as reported by Song et al. [67]. Notably, XEP-50 has a higher molecular weight than XEP-90 but does not have the same free radical scavenging capacity as XEP-90, which may be related to the different monosaccharide compositions; the contents of galactose, rhamnose and arabinose in the monosaccharide composition may have an effect on the antioxidant capacity, as reported by Kang et al. [68]. This may have an effect on the antioxidant capacity of both plants. In summary, the antioxidant capacity of polysaccharides is determined by a combination of factors, and it is difficult to explain the complex mechanism from a single factor. Therefore, the relationship between the antioxidant activity of XEP and its structure needs to be further investigated.

LX-2 is a cell lineage of hepatic stellate cells (HSCs) that is closely associated with the health status of the liver. HSCs are activated following stimulation or injury, and activated HSCs undergo morphological and functional changes, eventually transforming into fibroblasts or myofibroblasts while leading to liver fibrosis, which may further contribute to cirrhosis and liver cancer [69]. There are many factors that can activate and damage HSCs, such as ROS, inflammatory factors and lipid peroxidation. However, many of the different factors that cause liver damage are accompanied by increased oxidation and reduced antioxidant capacity [2]. Therefore, it is logical to use a natural antioxidant to help counteract the oxidative stress produced by hepatocytes

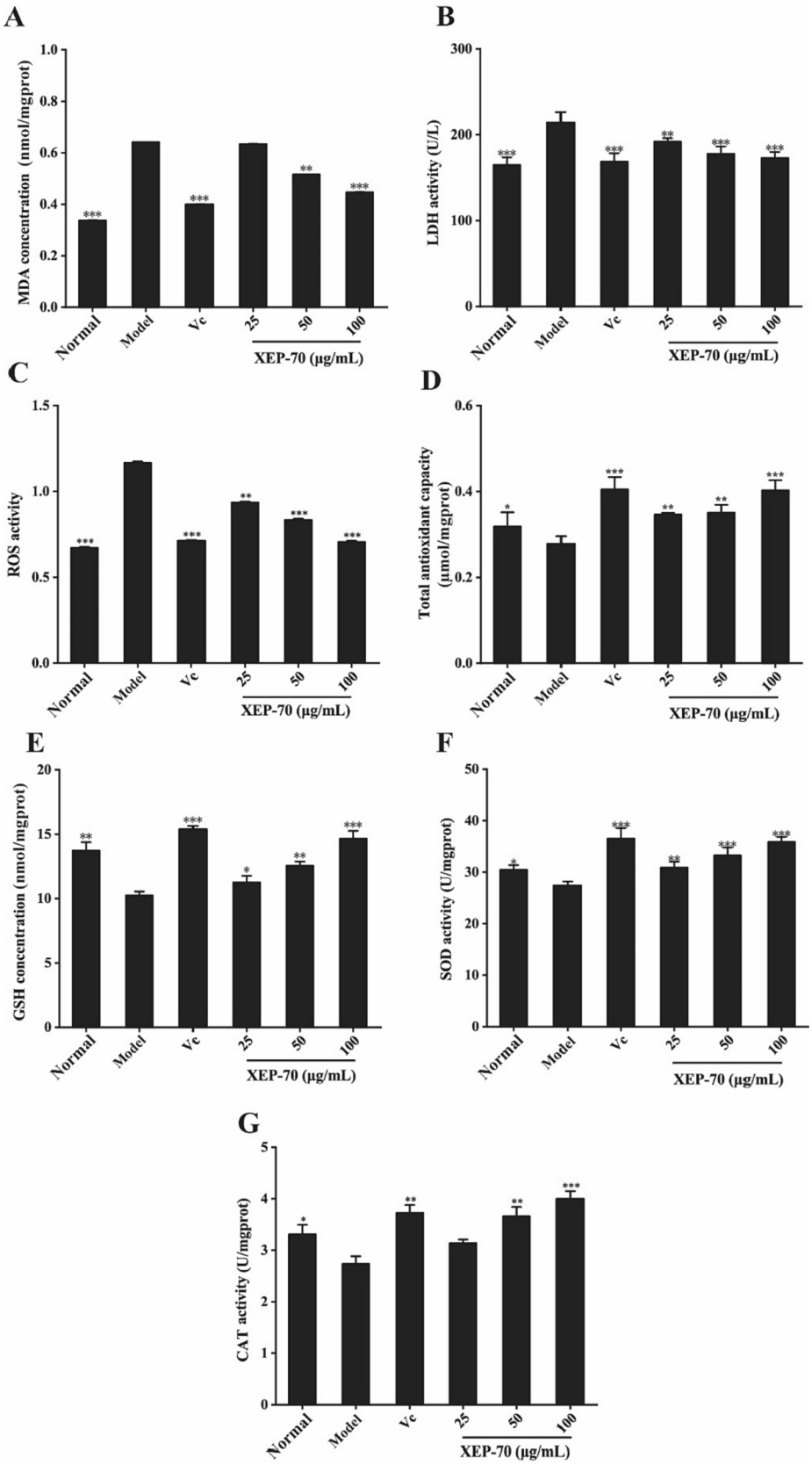

Fig. 5. Effect of XEP-70 on oxidative stress levels and antioxidant enzyme activities in H_2O_2-injured LX-2 cells. (A) MDA; (B) LDH; (C) ROS; (D) T-AOC; (E) GSH; (F) SOD; (G) CAT. Normal: untreated control cells. Model: Cells were treated with blank medium for 24 h and then treated with medium containing 30 μg/mL H_2O_2 for 24 h. Other groups: cells were treated with medium containing Vc or XEP-70 for 24 h and then treated with medium containing 30 μg/mL H_2O_2 for 24 h. All the data are expressed as the means ± SDs ($n = 6$). *p < 0.05, **$p < 0.01$ and ***$p < 0.001$ *vs.* the Model control group.

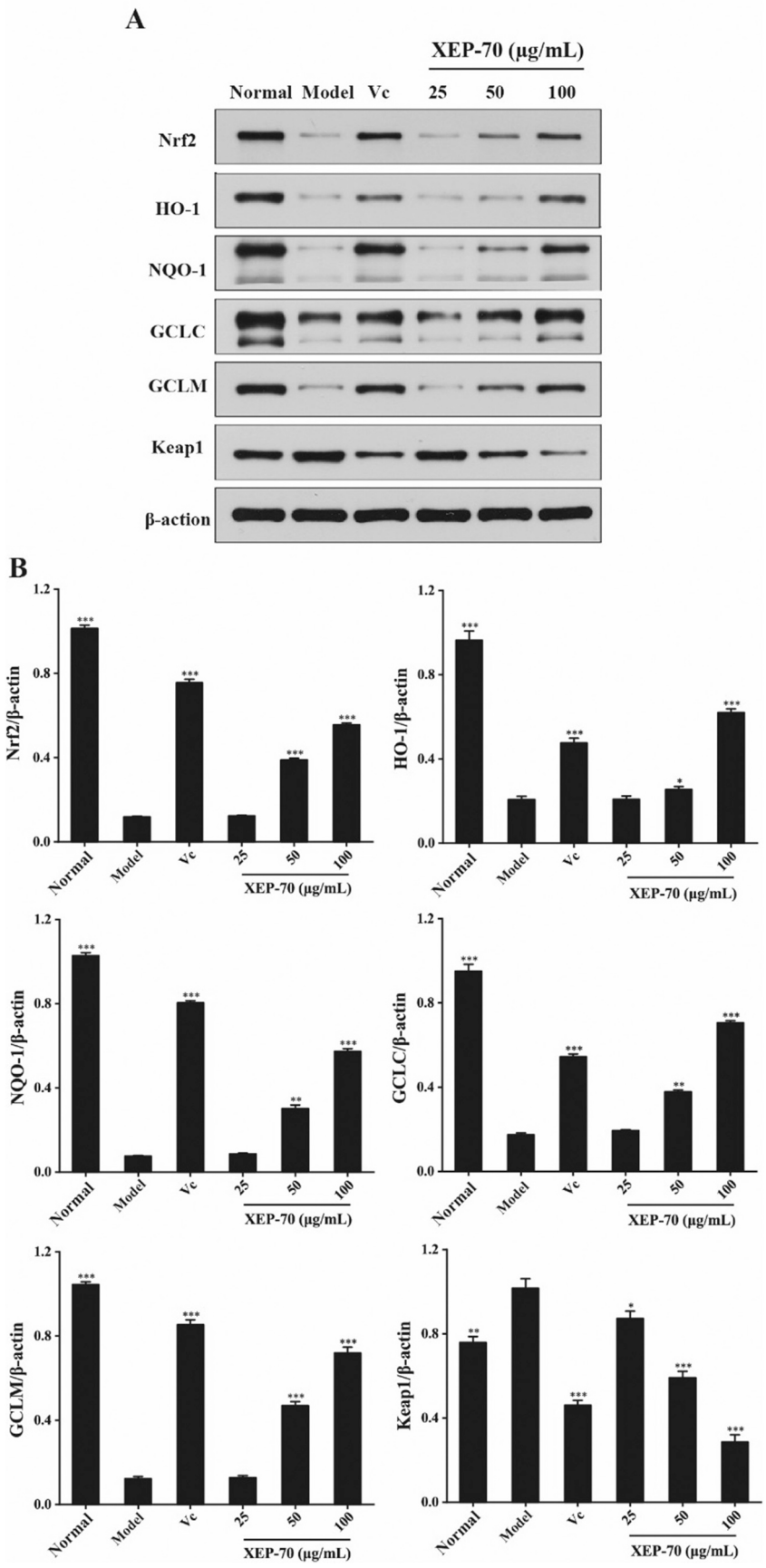

Fig. 6. Effect of XEP-70 on the protein expression of Nrf2, HO-1, NQO-1, GCLC, GCLM and Keap1 in H_2O_2-injured LX-2 cells.

and reduce the potential for oxidative damage, thus protecting the liver.

ROS consist of many different chemicals, among which hydrogen peroxide, which is stable and free from diffusion, is often used to study the oxidative stress response of cells [13–16,69]. Hydrogen peroxide has emerged as a major redox metabolite involved in redox sensing, signaling and redox regulation. The generation, transport and capture of H_2O_2 in biological settings as well as its biological consequences can now be addressed. Recent studies revealed that higher concentrations of H_2O_2 lead to adaptive stress responses *via* master switches such as Nrf2/Keap1 or NF-κB. Supraphysiologic concentrations of H_2O_2 (> 100 nM) can lead to damage of biomolecules, denoted as oxidative distress [70,71]. In the present study, H_2O_2 was applied to induce oxidative stress, as many previous studies have suggested that H_2O_2 is a highly reactive oxygen species that can diffuse throughout mitochondria and across cell membranes, causing many types of cellular injury; therefore, H_2O_2 seems to be a suitable agent for investigating reactive oxygen metabolite-induced hepatocellular oxidative damage. H_2O_2 can be metabolized to several ROS, including hydroxyl radicals, which are considered to be the most dangerous compounds to organisms. An excess of uneliminated H_2O_2 and its metabolites can oxidize virtually all types of macromolecules, including carbohydrates, nucleic acids, lipids and proteins. Increased levels of ROS overwhelm antioxidant defenses and subsequently lead to a state of oxidative stress, which may further impair body function and result in clinical deterioration [70–73]. The present data indicated that H_2O_2 inhibited CAT, SOD, and T-AOC activities, caused a substantial reduction in GSH content and increased MDA levels, suggesting a significant disruption in the oxidative balance after exposure to H_2O_2 treatment. In the present study, the protective effect of XEP-70 on H_2O_2-induced oxidative damage caused by LX-2 cells was investigated by preaddition of different concentrations of XEP-70 to the experimental group. XEP-70 at concentrations of 50 and 100 μg/mL significantly increased the activities of various antioxidant enzymes while significantly reducing the levels of MDA, LDH and ROS ($p < 0.05$).

Nrf2 is a basic “cap and collar” leucine zipper transcription factor that regulates the environmental stress response by regulating the expression of genes encoding antioxidants and detoxifying enzymes. The Nrf2-directed environmental stress response protects cells against a variety of stressors, including environmental pollutants such as electrophiles and oxidizing agents, immunotoxicants, and inflammatory agents [74,75]. Keap1, a cysteine-rich protein that acts as a substrate adaptor for the ubiquitination of Nrf2 by the Cul3-Rbx1 E3 ubiquitin ligase complex, targets Nrf2 for proteasomal degradation and maintains the transcription factor at a low level under nonstress conditions. Under oxidative stress and in the presence of excess ROS, the oxidation or conjugation of key cysteine residues in Keap1 increases, and the modification of Keap1 generally weakens its activity as an E3 ligase adaptor. The net effect of such Keap1 modification is disrupted; thus, c is no longer degraded in the cytosol and translocates into the nucleus and induces transcription of its target genes [76–78]. In the present study, supraphysiological concentrations of H_2O_2 (30 mM) produced a large amount of ROS in LX-2 cells, which led to a significant decrease in the expression of Nrf2 and a remarkable increase in the expression of Keap1, as well as a significant decrease in the expression of downstream antioxidant proteins, including NQO1, HO-1, GCLC and GCLM. However, pretreatment with XEP-70 for 24 h significantly increased Nrf2 expression and decreased Keap1 expression, allowing Nrf2 to bind to ARE elements and further promoting the significant expression of downstream antioxidant proteins, such as NQO1, HO-1, GCLC and GCLM ($P < 0.05$), thereby maintaining cellular activity and enhancing the antioxidant capacity of LX-2 cells. These findings suggested that XEP-70 may have some potential protective effects against oxidative damage in hepatocytes by activating the Nrf2/Keap1/ARE signaling pathway. However, this study is supported by only *in vitro* characterization. Further efforts need to be made to characterize these polysaccharides *in vivo* by using a suitable animal model of liver disease.

5. Conclusions

Three mannose-containing heteropolysaccharide fractions (XEP-50, XEP-70 and XEP-90) were isolated from *X. elegans*, in which XEP-70 exhibited the best antioxidant activity in free radical scavenging capacity and reducing power assays. Structural studies showed that XEP-70 was composed mainly of (1 → 4)-linked and (1 → 4,6)-linked α-D-Glc*p*, (1 → 4)-linked α-D-Gal*p*A, (1 → 2)-linked, (1 → 6)-linked and (1 → 2,6)-linked α-D-Man*p*, and (1 → 6)-linked and (1 → 2,6)-linked β-D-Gal*f*. Bioactivity analysis revealed that XEP-70 could effectively protect LX-2 cells against H_2O_2-induced oxidative damage by enhancing cellular antioxidant capacity by activating the Nrf2/Keap1/ARE signaling pathway. Thus, XEP-70 has good potential to protect hepatic stellate cells against oxidative damage.

Ethics statement

Not applicable.

Funding

This work was supported by the “Western Youth Scholars” Key Project (2021) of the Chinese Academy of Sciences, the “Kunlun elite high-end innovation and entrepreneurship talent program” of Qinghai Province, the Innovation Platform Program of Qinghai Province (2021-ZJ-T02) and the Key Project of the Chinese Academy of Sciences (Grant No. ZDRW-ZS-2020-2).

CRediT authorship contribution statement

Zheng Zhou: Writing – original draft, Project administration, Investigation. **Guoqiang Li:** Project administration, Investigation, Data curation. **Liang Gao:** Writing – original draft, Project administration, Data curation. **Yubi Zhou:** Writing – original draft, Supervision. **Yuancan Xiao:** Supervision, Conceptualization. **Hongtao Bi:** Writing – review & editing, Supervision, Funding acquisition. **Hongxia Yang:** Writing – review & editing, Supervision, Resources, Methodology, Funding acquisition.

Declaration of competing interest

The authors declare that they have no known competing financial interests or personal relationships that could have appeared to influence the work reported in this paper.

Data availability

The raw data supporting the conclusions of this article will be made available by the authors without undue reservation.

References

[1] J. Flieger, W. Flieger, J. Baj, R. Maciejewski, Antioxidants: classification, natural sources, activity/capacity measurements, and usefulness for the synthesis of nanoparticles, Materials 14 (2021) 4135.
[2] H. Cichoz-Lach, A. Michalak, Oxidative stress as a crucial factor in liver diseases, World J. Gastroenterol. 20 (25) (2014) 8082–8091.
[3] S. Li, H.Y. Tan, N. Wang, Z.J. Zhang, L. Lao, C.W. Wong, Y. Feng, The role of oxidative stress and antioxidants in liver diseases, Int. J. Mol. Sci. 16 (11) (2015) 26087–26124.
[4] Q. Chu, M. Chen, D. Song, X. Li, Y. Yang, Z. Zheng, Y. Li, Y. Liu, L. Yu, Z. Hua, X. Zheng, Apios americana Medik flowers polysaccharide (AFP-2) attenuates H(2)O (2) induced neurotoxicity in PC12 cells, Int. J. Biol. Macromol. 123 (2019) 1115–1124.
[5] D.K. Ingawale, S.K. Mandlik, S.R. Naik, Models of hepatotoxicity and the underlying cellular, biochemical and immunological mechanism(s): a critical discussion, Environ. Toxicol. Pharmacol. 37 (1) (2014) 118–133.
[6] S. Seen, Chronic liver disease and oxidative stress - a narrative review, Expert Rev. Gastroent. 15 (2021) 1021–1035.

[7] S. Li, X. Zhou, R. Chen, Q. Zhang, Y. Sun, H. Chen, Effect of natural polysaccharides on alcoholic liver disease: a review, Int. J. Biol. Macromol. 251 (2023) 126317.
[8] Y. Yuan, L. Che, C. Qi, Z. Meng, Protective effects of polysaccharides on hepatic injury: a review, Int. J. Biol. Macromol. 141 (2019) 822–830.
[9] S.L. Li, H.R. Li, X.D. Xu, P.E. Saw, L. Zhang, Nanocarrier-mediated antioxidant delivery for liver diseases, Theranostics 10 (2020) 1262–1280.
[10] J. Xie, M. Jin, G.A. Morris, X. Zha, H. Chen, Y. Yi, J. Li, Z. Wang, J. Gao, S. Nie, P. Shang, M. Xie, Advances on bioactive polysaccharides from medicinal plants, Crit. Rev. Food Sci. 56 (2016) S60–S84.
[11] S. Ullah, A.A. Khalil, F. Shaukat, Y. Song, Sources, extraction and biomedical properties of polysaccharides, Foods 8 (2019) 304.
[12] S.R.N. Bo, M. Zhang, M. Dan, The traditional use, structure, and immunostimulatory activity of bioactive polysaccharides from traditional Chinese root medicines: a review, Heliyon 10 (2024) e23593.
[13] G. Huang, X. Mei, J. Hu, The antioxidant activities of natural polysaccharides, Curr. Drug Targets 18 (2017) 1296–1300.
[14] L. Bai, D. Xu, Y. Zhou, Y. Zhang, H. Zhang, Y. Chen, Y. Cui, Antioxidant activities of natural polysaccharides and their derivatives for biomedical and medicinal applications, Antioxidants 11 (2022) 2491.
[15] O.P.N. Yarley, A.B. Kojo, C.S. Zhou, X.J. Yu, A. Gideon, H.H. Kwadwo, O. Richard, Reviews on mechanisms of in vitro antioxidant, antibacterial and anticancer activities of water-soluble plant polysaccharides, Int. J. Biol. Macromol. 183 (2021) 2262–2271.
[16] P.A.R. Fernandes, M.A. Coimbra, The antioxidant activity of polysaccharides: a structure-function relationship overview, Carbohydr. Polym. 314 (2023) 120965.
[17] J.H. Luo, J. Li, Z.C. Shen, X.F. Lin, A.Q. Chen, Y.F. Wang, E.S. Gong, D. Liu, Q. Zou, X.Y. Wang, Advances in health-promoting effects of natural polysaccharides: regulation on Nrf2 antioxidant pathway, Front. Nutr. 10 (2023) 1102146.
[18] T. Spribille, P. Resl, D.E. Stanton, G. Tagirdzhanova, Evolutionary biology of lichen symbioses, New Phytol. 234 (2022) 1566–1582.
[19] H. Turkez, E. Aydin, A. Aslan, *Xanthoria elegans* (link) (lichen) extract counteracts DNA damage and oxidative stress of mitomycin C in human lymphocytes, Cytotechnology 64 (2012) 679–686.
[20] E. Aydin, H. Türkez, Effects of lichenic extracts (*Bryoria capillaris*, *Peltigera rufescens* and *Xanthoria elegans*) on human blood cells: a cytogenetic and biochemical study, Fresen. Environ. Bull. 20 (2011) 2992–2998.
[21] J. Kumar, P. Dhar, A.B. Tayade, D. Gupta, O.P. Chaurasia, D.K. Upreti, R. Arora, R. B. Srivastava, Antioxidant capacities, phenolic profile and cytotoxic effects of saxicolous lichens from trans-Himalayan cold desert of Ladakh, PloS One 9 (2014) e98696.
[22] A.K. Gautam, D. Yadav, S.S. Bhagyawant, P.K. Singh, J.O. Jin, Lichen: a comprehensive review on lichens as a natural sources exploring nutritional and biopharmaceutical benefits, Prog. Nutr. 23 (2021) e2021153.
[23] J. Boustie, S. Tomasi, M. Grube, Bioactive lichen metabolites: alpine habitats as an untapped source, Phytochem. Rev. 10 (2011) 287–307.
[24] S. Zha, Q. Zhao, J. Chen, L. Wang, G. Zhang, H. Zhang, B. Zhao, Extraction, purification and antioxidant activities of the polysaccharides from maca (Lepidium meyenii), Carbohydr. Polym. 111 (2014) 584–587.
[25] Z. Zhang, X. Wang, X. Mo, H. Qi, Degradation and the antioxidant activity of polysaccharide from Enteromorpha linza, Carbohydr. Polym. 92 (2013) 2084–2087.
[26] R. Zhu, X. Zhang, Y. Wang, L. Zhang, J. Zhao, G. Chen, J. Fan, Y. Jia, F. Yan, C. Ning, Characterization of polysaccharide fractions from fruit of *Actinidia arguta* and assessment of their antioxidant and antiglycated activities, Carbohydr. Polym. 210 (2019) 73–84.
[27] N. Wang, G. Jia, X. Wang, Y. Liu, Z. Li, H. Bao, Q. Guo, C. Wang, D. Xiao, Fractionation, structural characteristics and immunomodulatory activity of polysaccharide fractions from asparagus (*asparagus officinalis* L.) skin, Carbohydr. Polym. 256 (2021) 117514.
[28] H.L. Zhang, S.H. Cui, X.Q. Zha, V. Bansal, L. Xue, X.L. Li, R. Hao, L.H. Pan, J.P. Luo, Jellyfish skin polysaccharides: extraction and inhibitory activity on macrophage-derived foam cell formation, Carbohydr. Polym. 106 (2014) 393–402.
[29] G. Zhang, C. Liu, R. Zhang, A novel acidic polysaccharide from blackened jujube: structural features and antitumor activity in vitro, Front. Nutr. 9 (2022) 1001334.
[30] F. Yue, J. Zhang, J. Xu, T. Niu, X. Lu, M. Liu, Effects of monosaccharide composition on quantitative analysis of total sugar content by phenol-sulfuric acid method, Front. Nutr. 9 (2022) 963318.
[31] L. Rong, G. Li, Y. Zhang, Y. Xiao, Y. Qiao, M. Yang, L. Wei, H. Bi, T. Gao, Structure and immunomodulatory activity of a water-soluble alpha-glucan from *Hirsutella sinensis* mycelia, Int. J. Biol. Macromol. 189 (2021) 857–868.
[32] R. Hou, Q. Li, J. Liu, Y. Hu, Selenylation modification of Atractylodes macrocephala polysaccharide and evaluation of antioxidant activity, Adv. Polym. Technol. 2019 (2019) 1–8.
[33] X. Huang, J. Ma, L. Wei, J. Song, C. Li, H. Yang, Y. Du, T. Gao, H. Bi, An antioxidant α-glucan from *Cladina rangiferina* (L) Nyl. And its protective effect on alveolar epithelial cells from Pb^{2+}-induced oxidative damage, Int. J. Biol. Macromol. 112 (2018) 101–109.
[34] M. Zhang, J. Ma, H. Bi, J. Song, H. Yang, Z. Xia, Y. Du, T. Gao, L. Wei, Characterization and cardioprotective activity of anthocyanins from Nitraria tangutorum Bobr. By-products, Food Funct. 8 (2017) 2771–2782.
[35] Y. Qin, L. Xiong, M. Li, J. Liu, H. Wu, H. Qiu, H. Mu, X. Xu, Q. Sun, Preparation of bioactive polysaccharide nanoparticles with enhanced radical scavenging activity and antimicrobial activity, J. Agric. Food Chem. 66 (2018) 4373–4383.
[36] B. Zeng, M. Su, Q. Chen, Q. Chang, W. Wang, H. Li, Antioxidant and hepatoprotective activities of polysaccharides from Anoectochilus roxburghii, Carbohydr. Polym. 153 (2016) 391–398.
[37] R. Hou, T. Xu, Q. Li, F. Yang, C. Wang, T. Huang, Z. Hao, Polysaccharide from Echinacea purpurea reduce the oxidant stress in vitro and in vivo, Int. J. Biol. Macromol. 149 (2020) 41–50.
[38] Q. Wu, C. Liu, J. Zhang, W. Xiao, F. Yang, Y. Yu, T. Li, Y. Wang, Schisandra chinensis polysaccharide protects against cyclosporin A-induced liver injury by promoting hepatocyte proliferation, J. Funct. Foods 87 (2021) 104799.
[39] X. Meng, H. Kuang, Q. Wang, H. Zhang, D. Wang, T. Kang, A polysaccharide from Codonopsis pilosula roots attenuates carbon tetrachloride-induced liver fibrosis via modulation of TLR4/NF-κB and TGF-β1/Smad3 signaling pathway, Int. Immunopharmacol. 119 (2023) 110180.
[40] Q. Wu, C. Liu, J. Zhang, W. Xiao, F. Yang, Y. Yu, T. Li, Y. Wang, Schisandra chinensis polysaccharide protects against cyclosporin A-induced liver injury by promoting hepatocyte proliferation, J. Funct. Foods 87 (2021) 104799.
[41] Y. Choi, K. Yu, M. Kim, B. Kwon, I. Park, Y. Choo, S. Kim, S. Jeong, J. Kim, J. Kim, The extract of edible alga *Petalonia binghamiae* suppresses TGF-β1-H_2O_2-induced liver fibrogenesis in LX-2 and HepG2 cells, Nat. Prod. Commun. 13 (2018) 757–759.
[42] M. Shang, H. Sun, Y. Wu, Y. Gong, Z. Tang, F. Meng, L. He, X. Yu, Y. Huang, X. Li, In vivo and in vitro studies using Clonorchis sinensis adult-derived total protein (CsTP) on cellular function and inflammatory effect in mouse and cell model, Parasitol. Res. 119 (2020) 1641–1652.
[43] M. Yang, X. Lin Rong, G. Zhang, Q. Li, C. Wang, Y. Li, L. Xiao, H. Bi Wei, *Hirsutella sinensis* mycelium polysaccharides attenuate the TGF-β1-induced epithelial-mesenchymal transition in human intrahepatic bile duct epithelial cells, Int. J. Biol. Macromol. 254 (2024) 127834.
[44] S. Li, A. Gao, S. Dong, Y. Chen, S. Sun, Z. Lei, Z. Zhang, Purification, antitumor and immunomodulatory activity of polysaccharides from soybean residue fermented with Morchella esculenta, Int. J. Biol. Macromol. 96 (2017) 26–34.
[45] M. Wu, H. Feng, J. Song, L. Chen, Z. Xu, W. Xia, W. Zhang, Structural elucidation and immunomodulatory activity of a neutral polysaccharide from the Kushui rose (Rosa setate x Rosa rugosa) waste, Carbohydr. Polym. 232 (2020) 115804.
[46] M. Tabarsa, S. You, K. Yelithao, S. Palanisamy, N.M. Prabhu, M. Nan, Isolation, structural elucidation and immuno-stimulatory properties of polysaccharides from Cuminum cyminum, Carbohydr. Polym. 230 (2020) 115636.
[47] H. Zhang, P. Zou, H. Zhao, J. Qiu, J.M. Regenstein, X. Yang, Isolation, purification, structure and antioxidant activity of polysaccharide from pinecones of *Pinus koraiensis*, Carbohydr. Polym. 251 (2021) 117078.
[48] J. Chen, X. Zhang, D. Huo, C. Cao, Y. Li, Y. Liang, B. Li, L. Li, Preliminary characterization, antioxidant and alpha-glucosidase inhibitory activities of polysaccharides from *Mallotus furetianus*, Carbohydr. Polym. 215 (2019) 307–315.
[49] G. Ye, J. Li, J. Zhang, H. Liu, Q. Ye, Z. Wang, Structural characterization and antitumor activity of a polysaccharide from *Dendrobium wardianum*, Carbohydr. Polym. 269 (2021) 118253.
[50] P. He, Z. Dong, Q. Wang, Q.-P. Zhan, M.-M. Zhang, H. Wu, Structural characterization and immunomodulatory activity of a polysaccharide from *Eurycoma longifolia*, J. Nat. Prod. 82 (2019) 169–176.
[51] Z.N. Cai, W. Li, S. Mehmood, W.J. Pan, Y. Wang, F.J. Meng, X.F. Wang, Y.M. Lu, Y. Chen, Structural characterization, in vitro and in vivo antioxidant activities of a heteropolysaccharide from the fruiting bodies of *Morchella esculenta*, Carbohydr. Polym. 195 (2018) 29–38.
[52] F. Gao, L. Luo, L. Zhang, A new galactoglucomannan from the mycelium of the medicinal parasitic fungus Cordyceps cicadae and its immunomodulatory activity in vitro and in vivo, Molecules 28 (2023) 3867.
[53] Q. Guo, L. Xu, Y. Chen, Q. Ma, R.K. Santhanam, Z. Xue, X. Gao, H. Chen, Structural characterization of corn silk polysaccharides and its effect in H_2O_2 induced oxidative damage in L6 skeletal muscle cells, Carbohydr. Polym. 208 (2019) 161–167.
[54] Z.M. Rashid, M. Mormann, K. Steckhan, A. Peters, S. Esch, A. Hensel, Polysaccharides from lichen Xanthoria parietina: 1,4/1,6-alpha-d-glucans and a highly branched galactomannan with macrophage stimulating activity via Dectin-2 activation, Int. J. Biol. Macromol. 134 (2019) 921–935.
[55] G. Shrestha, L.L. St, K.L. O'Neill Clair, The immunostimulating role of lichen polysaccharides: a review, Phytother. Res. 29 (2014) 317–322.
[56] Y.Q. Du, Y. Liu, J.H. Wang, Polysaccharides from *Umbilicaria esculenta* cultivated in Huangshan Mountain and immunomodulatory activity, Int. J. Biol. Macromol. 72 (2015) 1272–1276.
[57] X. Wang, J.Y. Yu, Y. Sun, H. Wang, H. Shan, S. Wang, Baicalin protects LPS-induced blood-brain barrier damage and activates Nrf2-mediated antioxidant stress pathway, Int. Immunopharmacol. 96 (2021) 107725.
[58] L. Zhu, S. He, L. Huang, D. Ren, T. Nie, K. Tao, L. Xia, F. Lu, Z. Mao, Q. Yang, Chaperone-mediated autophagy degrades Keap1 and promotes Nrf2-mediated antioxidative response, Aging Cell 21 (2022) e13616.
[59] S.K. Chiang, S.E. Chen, L.C. Chang, The role of HO-1 and its crosstalk with oxidative stress in cancer cell survival, Cells 10 (2021) 2401.
[60] A.L. Pey, C.F. Megarity, D.J. Timson, NAD(P)H quinone oxidoreductase (NQO1): an enzyme which needs just enough mobility, in just the right places, Biosci. Rep. 39 (2019) BSR20180459.
[61] C.M. Schaupp, D. Botta, C.C. White, D.K. Scoville, S. Srinouanprachanh, T. K. Bammler, J. MacDonald, T.J. Kavanagh, Persistence of improved glucose homeostasis in Gclm null mice with age and cadmium treatment, Redox Biol. 49 (2022) 102213.
[62] T. Spribille, V. Tuovinen, P. Resl, D. Vanderpool, H. Wolinski, M.C. Aime, K. Schneider, E. Stabentheiner, M. Toome-Heller, G. Thor, H. Mayrhofer, H. Johannesson, J.P. McCutcheon, Basidiomycete yeasts in the cortex of ascomycete macrolichens, Science 353 (2016) 488–492.

[63] O.T. Adenubi, I.M. Famuyide, L.J. McGaw, J.N. Eloff, Lichens: an update on their ethnopharmacological uses and potential as sources of drug leads, J. Ethnopharmacol. 298 (2022) 115657.
[64] X. Chen, R. Tang, T. Liu, W. Dai, Q. Liu, G. Gong, S. Song, M. Hu, L. Huang, Z. Wang, Physicochemical properties, antioxidant activity and immunological effects in vitro of polysaccharides from *Schisandra sphenanthera* and *Schisandra chinensis*, Int. J. Biol. Macromol. 131 (2019) 744–751.
[65] S.Q. Huang, S. Ding, L. Fan, Antioxidant activities of five polysaccharides from *Inonotus obliquus*, Int. J. Biol. Macromol. 50 (2012) 1183–1187.
[66] H. Song, Q. Zhang, Z. Zhang, J. Wang, In vitro antioxidant activity of polysaccharides extracted from *Bryopsis plumosa*, Carbohydr. Polym. 80 (2010) 1057–1061.
[67] M.C. Kang, S.Y. Kim, E.A. Kim, J.H. Lee, Y.S. Kim, S.K. Yu, J.B. Chae, I.H. Choe, J. H. Cho, Y.J. Jeon, Antioxidant activity of polysaccharide purified from Acanthopanax koreanum Nakai stems in vitro and in vivo zebrafish model, Carbohydr. Polym. 127 (2015) 38–46.
[68] V. Hernandez-Gea, S.L. Friedman, Pathogenesis of liver fibrosis, Annu. Rev. Pathol. 6 (2011) 425–456.
[69] K. Jomova, R. Raptova, S.Y. Alomar, S.H. Alwasel, E. Nepovimova, K. Kuca, M. Valko, Reactive oxygen species, toxicity, oxidative stress, and antioxidants: chronic diseases and aging, Arch. Toxicol. 97 (2023) 2499–2574.
[70] H. Sies, Hydrogen peroxide as a central redox signaling molecule in physiological oxidative stress: oxidative eustress, Redox Biol. 11 (2017) 613–619.
[71] K. Aschbacher, A. O'Donovan, O.M. Wolkowitz, F.S. Dhabhar, Y. Su, E. Epel, Good stress, bad stress and oxidative stress: insights from anticipatory cortisol reactivity, Psychoneuroendocrinology 38 (2013) 1698–1708.
[72] V.I. Lushchak, Free radicals, reactive oxygen species, oxidative stress and its classification, Chem. Biol. Interact. 224C (2014) 164–175.
[73] F. Ursini, M. Maiorino, H.J. Forman, Redox homeostasis: the golden mean of healthy living, Redox Biol. 8 (2016) 205–215.
[74] S. Fourquet, R. Guerois, D. Biard, M.B. Toledano, Activation of NRF2 by nitrosative agents and H2O2 involves KEAP1 disulfide formation, J. Biol. Chem. 285 (2010) 8463–8471.
[75] J. Yin, J. Duan, Z. Cui, W. Ren, T. Li, Y. Yin, Hydrogen peroxide-induced oxidative stress activates NF-κB and Nrf2/Keap1 signals and triggers autophagy in piglets, RSC Adv. 5 (2015) 15479–15486.
[76] Y. Song, Y. Qu, C. Mao, R. Zhang, D. Jiang, X. Sun, Post-translational modifications of Keap1: the state of the art, Front. Cell Dev. Biol. 11 (2024) (2023) 1332049 doi: 10.3389/fcell.2023.1332049.eCollection.
[77] K.M. Pensabene, J. LaMorte, A.E. Allender, J. Wehr, P. Kaur, M. Savage, A. L. Eggler, Acute oxidative stress can paradoxically suppress human NRF2 protein synthesis by inhibiting global protein translation, Antioxidants (Basel) 12 (2023) 1735.
[78] M. Hammad, M. Raftari, R. Cesário, R. Salma, P. Godoy, S.N. Emami, S. Haghdoost, Roles of oxidative stress and Nrf2 signaling in pathogenic and non-pathogenic cells: a possible general mechanism of resistance to therapy, Antioxidants (Basel) 12 (2023) 1371.